Modification of self-assembled nanotubes by click chemistry generates new nanotubes by an out-of equilibrium process

Thi-Thanh-Tam Nguyen, François-Xavier Simon,† Jérôme Combet, Marc Schmutz and Philippe J. Mésini*

Received 12th August 2010, Accepted 8th November 2010
DOI: 10.1039/c0sm00810a

An aromatic diamide compound self-assembles in non-polar solvents to form nanotubes with diameters of 27 nm. We have synthesized different analogues of this compound and we found that the ones bearing an alkyne or an azide group are still able to form nanotubes with diameters of the same order. The functional groups offered the possibility to perform copper catalyzed alkyne and azide cycloadditions (CuAACs), which were achieved directly on the self-assembled tubes. The reaction yielded new nanotubes with similar dimensions to the starting ones, as shown by freeze fracture electron microscopy and SAXS. Chemical analysis of those tubes shows that they are composed mainly of the reacted molecules. When these new nanotubes are dissociated by heat they cannot be re-assembled from their constituting molecules, which shows that they do not result from a conventional reversible self-assembly at equilibrium.

Introduction

In material science, the discovery of the carbon nanotubes (CNTs),[1–3] with unique shape, monodimensionality and high aspect ratio, has allowed to envision new applications with those nanoobjects.[4] However, many applications require the surface functionalization of the tubes with appropriate chemical groups, as in the case of sensors or drug delivery systems.[5,6] This modification is necessary at least to solubilize or compatibilize them.[7] It requires many synthetic efforts and development of a specific methodology;[8] moreover, identification of the products and quantification of the reaction are often difficult. Beside the CNTs, many efforts have been pursued to develop nanotubes made from self-assembly of small compounds. These objects have several features that make them attracting for applications: they are easy to form, through spontaneous self-assembly; they are pure, because the constituting molecules are purified by standard methods before self-assembly; and their thermoreversibility facilitates their processability. The functionalization of the tubes may be considered easier than that of CNTs since it can be performed on the constituting molecules before self-assembly by standard synthetic methods. Indeed, some functional tubes have been designed to bind ligands, enantioselectively,[9] or proteins.[10,11] But these examples are still rare. Generally, when a compound forming nanotubes is chemically modified, even slightly, the resulting analogues can no longer form tubes: they form either self-assemblies with different shapes or precipitate or they become totally soluble. This behavior shows that the formation of the tubes is the result of a fragile combination of interactions and packing that are easily unbalanced by the introduction of new groups onto the molecules. But it is almost impossible to predict whether a given chemical structure can form tubes. This is mainly because the structures of the self-assembled tubes at the molecular level are known only in a few cases.[12,13] Theoretical models for the self-assembly of nanotubes have been proposed[14–18] by physicists but they rely on a phenomenological description of the energies of the self-assemblies. They do not take into account the local packing or interactions between the molecules and cannot identify the molecular parameters that govern the formation of the tubes.

Herein, we explore the possibility of functionalizing directly self-assembled organic nanotubes that are reactive. We have previously shown[19] that the diamide **1** (Scheme 1) is able to self-assemble in alkanes to form nanotubes with outer diameters of 29 nm and lengths of several micrometres. We have recently described[20] the synthesis of the analogues **2** and **3** bearing, respectively, an alkyne and an azide group. Both groups can react, respectively, with azides and alkynes by copper catalyzed cycloaddition of alkynes and azides (CuAAC).[21,22] We have shown that these new analogues are also able to form nanotubes in alkanes, and we perform CuAAC reactions directly on these reactive tubes once they are self-assembled. The present paper extends this reaction to new compounds. The aggregates produced by the reaction have been studied to determine their chemical composition and their shape. The use of SAXS has been used to confirm the tubular shape of some aggregates and to compare accurately their dimensions before and after reaction.

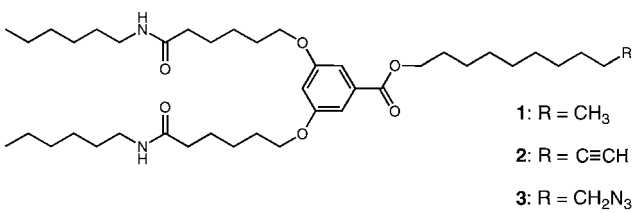

Scheme 1 Chemical structure of the self-assembling compounds.

Institut Charles Sadron, CNRS, 23 rue du Loess, BP 84047, 67034 Strasbourg Cedex 2, France. E-mail: mesini@ics.u-strasbg.fr; Fax: +33 (0)388 41 40 99; Tel: +33 (0)388 41 40 70
† Present address: BASF, 49 avenue Georges Pompidou, 92593 Levallois-Perret Cedex, France.

Materials and methods

Chemicals

Chemicals were bought from Aldrich or Acros and used as is. NMR spectra were recorded on a Bruker Avance 400 operating at 400 MHz for ^{1}H and 100 MHz for ^{13}C. The FTIR spectra were recorded on a Bruker Vertex 70 spectrometer equipped with an ATR diamond reflection unit (MVPStar). Mass spectra were recorded with a Bruker Daltonique microTOF operating with an electrospray source. Compounds **4** through **8** are products from the reactions with nanotubes, but were also synthesized independently by standard synthesis. Compounds **2**, **3**, **4**, **5**, **7**, azidodecane and 10-azidodecan-1-ol were synthesized as previously described.[20]

Syntheses of 6 and 8

3,5-Bis-(5-hexylcarbamoyl-pentyloxy)-benzoic acid 10-(4-decyl-3*H*-[1,2,3]triazol-1-yl)-decyl ester (6). A solution of **3** (100 mg, 0.14 mmol), 1-dodecyne (70 mg, 0.42 mmol, 3 equiv.), and $CuSO_4 \cdot 5H_2O$ (17 mg, 70 μmol, 0.5 equiv.) in 4 mL H_2O/THF (1 : 1, 4 mL) under Ar was treated by sodium ascorbate (28 mg, 0.14 mmol, 1 equiv.). The mixture was stirred at 25 °C. After 20 min, the medium demixed into 2 liquid phases and CH_3CN (2 mL) was added to homogenize the medium that was stirred for further 4 h. The solvents were removed under vacuum and the residue was chromatographed (SiO_2, MeOH/CH_2Cl_2 4/96 eluent) to afford a grey solid (105 mg, 87% yield). The compound was recrystallized from CH_3CN (50% yield). Mp 82.0 °C. δ_H (400 MHz, $CDCl_3$): 7.24 (s, Htriazole), 7.13 (d, 2H, *J* 2.0, C2–H, C6–H), 6.60 (t, 1H, *J* 2.2, C4–H), 5.50 (br s, 2H, NH), 4.27 (m, 4H, CH_2Ntriazole and $COOCH_2$), 3.97 (t, 4H, *J* 6.48, $ArOCH_2$), 3.24 (q, 4H, *J* 6.6, CH_2NHCO), 2.70 (t, 2H, *J* 7.7, CH_2Ctriazole), 2.19 (t, 4H, *J* 7.5, CH_2CONH), 1.87 (t, 2H, *J* 6.8, $COOCH_2CH_2$), 1.83–1.63 (m, 12H, CH_2CH_2Ctriazole, $ArOCH_2CH_2$, CH_2CH_2Ntriazole, $NHCOCH_2CH_2$), 1.52–1.50 (8H, $CONHCH_2CH_2$, CH_2CH_3), 1.30–1.25 (36H, CH_2), 0.87 (9H, CH_3); δ_C (100 MHz, $CDCl_3$): 173.0 (CONH), 166.8 (COO), 160.4 (C3, C5), 148.5 (CH_2Ctriazole), 132.6 (C1), 120.7 (CHtriazole), 108.1 (C2, C6), 106.5 (C4), 68.3 ($ArOCH_2$), 65.6 ($ArCOOCH_2$), 50.5 (CH_2Ntriazole), 39.9 ($CONHCH_2$), 37.1 ($NHCOCH_2$), 32.2 ($CH_2(CH_2)_7$Ctriazole), 31.8 ($CONH(CH_2)_3CH_2$), 30.7 (CtriazoleCH_2CH_2), 30.03, 29.98, 29.93, 29.90, 29.85, 29.72, 29.67, 29.66, 29.6, 29.5, 29.3, 29.2, 30.0, 26.9, 26.10, 26.05, 25.8, 23.0, 22.9, 14.4 (CH_3), 14.3 (CH_3); ν_{max} (FTIR-ATR, diamond)/cm^{-1}: 3307 (ν NH), 3075 (ν CH_{ar}), 2955 (ν_{as} CH_3), 2923 (ν_{as} CH_2), 2870 (ν_s CH_3), 2853 (ν_s CH_2), 1714 (ν CO, ArCOO), 1638 (amide I), 1597 (ν C=C), 1541 (amide II), 1464 (δ CH_2), 1384, 1343, 1299 (amide III and triazole), 1240 (ν_{as} = C–O–C), 1170, 1067, 837, 764, 724, 680; *m*/*z* (ESI^+ HRMS) 896.7109 (MH^+, $C_{53}H_{93}N_5O_6$ requires 896.7199).

3,5-Bis-(5-hexylcarbamoyl-pentyloxy)-benzoic acid 10-(4-hydroxymethyl-3*H*-[1,2,3]triazol-1-yl)-decyl ester (8). 3 (49 mg, 67 μmol) was suspended in a solution of propargylic alcohol (57 mg, 1 mmol, 15 equiv.) in H_2O (5 mL) under Ar. Sodium ascorbate (10 mg, 50 μmol, 0.75 equiv.) and $CuSO_4 \cdot 5H_2O$ (14 mg, 56 μmol, 0.8 equiv.) were sequentially added and the medium became green. The mixture was stirred for 3 days at 25 °C and the solid was filtered, washed with water, and dissolved in CH_2Cl_2 (5 mL). The solution was dried ($MgSO_4$), evaporated under vacuum and the residue chromatographed (SiO_2, isopropanol/CH_2Cl_2 5/95 eluent) to afford pure **8** as a white solid (52.8 mg, quantitative). Mp 80.9 °C. δ_H (400 MHz, $CDCl_3$) 7.66 (br s, 1H, Htriazole), 7.13 (d, 2H, *J* 6.5, C2–H, C6–H), 6.60 (s, 1H, C4–H), 5.55 (br s, 2H, amide NH), 4.83 (br s, 2H, CtriazoleCH_2OH), 4.34 (br s, 2H, NtriazoleCH_2), 4.28 (t, 2H, *J* 6.5, $COOCH_2$), 3.96 (t, 4H, *J* 6.2, $ArOCH_2$), 3.23 (m, 4H, $CONHCH_2$), 2.80 (br s, 1H, OH), 2.19 (t, 4H, *J* 7.7, $NHCOCH_2$), 1.89 (br s, 2H, Ctriazole CH_2CH_2), 1.79–1.70 (m, 10H, $ArOCH_2CH_2$, $COOCH_2CH_2$, $NHCOCH_2CH_2$), 1.49–1.25 (m, 32H, CH_2), 0.87 (t, 6H, *J* 7.0, CH_3); δ_C (100 MHz, $CDCl_3$): 173.10 (CONH), 166.85 (COO), 160.35 (C3, C5), 147.2 (CtriazoleCH_2), 132.6 (C1), 108.1 (C2, C6), 106.1 (C4), 68.4 ($ArOCH_2$), 65.6 ($ArCOOCH_2$), 59.4 (CH_2OH), 57.0 (NtriazoleCH_2), 39.9 ($CONHCH_2$), 38.0, 37.0, 31.79 ($NHCOCH_2$), 29.96 ($CH_3CH_2CH_2$), 29.6, 29.2, 26.9, 26.1, 25.8, 22.9 (CH_2CH_3), 14.3 (CH_3); ν_{max} (FTIR-ATR, diamond)/cm^{-1} 3305 (broad, ν NH and ν OH), 3075 (ν CH_{Ar}), 2952 (ν_{as}, CH_3), 2924 (ν_{as}, CH_2), 2853 (ν_s, CH_2), 2360, 2341, 1726 (ArCOO, ν CO), 1639 (amide I), 1613, 1599, 1545 (amide II), 1466 (δ CH_2), 1384, 1347, 1300, 1228, 1175 (ν N–N), 1160, 1110, 1069, 618 cm^{-1}; *m*/*z* (ESI^+ HRMS) 792.5750 (MLi^+, $C_{44}H_{75}N_5O_7$ requires 792.5827).

Reaction with gels

2 (51 mg) was mixed with cyclohexane (2.5 g, 2 wt% of **2**) degassed with Ar in a vial tightly closed with a Teflon gasket and a screw cap. The mixture was heated until complete dissolution of the solid, allowed to cool at 25 °C and let stand until the formation of a gel. A saturated solution of $Cu(PPh_3)_3Br$ in cyclohexane was prepared by mixing the catalyst (66 mg, 71.5 μmol) with cyclohexane (2.2 g) and filtering off the undissolved solid. This solution was mixed with a solution of 10-azidodecan-1-ol (150 mg, 750 μmol) in C_6H_{12} (1.3 g). The resulting solution was layered on top of the **2**/cyclohexane gel, and let diffuse under Ar (Fig. 1). The diffusion of the copper species resulted in staining of the gel into a dark brown color.

The reaction solution was removed when the color frontline reached the bottom of the gel. The time required was about 1 week for a gel of 0.5 cm in height. The tube was opened and the

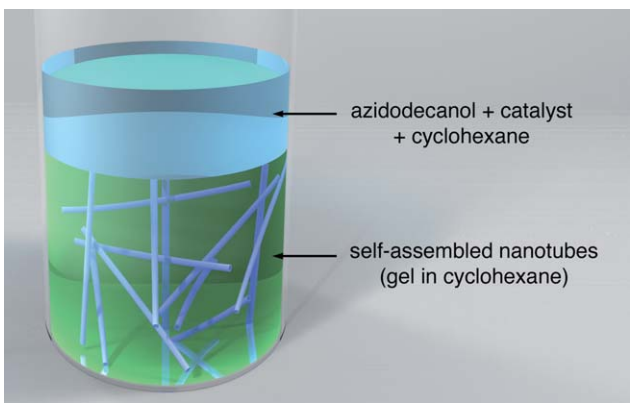

Fig. 1 Schematic experimental set-up for the reactions with self-assembled nanotubes.

top solution was removed with a pipette, and replaced by a solution of acetylacetone in cyclohexane (0.1 M, 7 mL). The solution was left on top of the gel for 24 h, then removed with a pipette and this step was repeated 5 times.

Electron microscopy

Small pieces were cut from the reacted gels (typically 2 × 2 × 2 mm), placed between two copper holders and rapidly frozen in liquid N_2. The samples were kept frozen while transferred in a home-made freeze fracture apparatus (developed by J.-C. Homo) where the holders were split opened to fracture the gels. Pt (2 nm) was evaporated on the samples under a 45° angle, then a reinforcing carbon layer (20 nm) under a 90° angle, respectively, to the surface. The sample was warmed up to room temperature and the replicas were carefully washed with chloroform and picked up onto 400 mesh grids. The grids were observed with a Philipps CM12 operating at 120 kV with a SIS Megaview III camera or a FEI tecnai G2 at 200 kV with a FEI eagle 2 k ssCCD camera.

Samples of the gel were taken at different heights to verify that the diffusion of the catalyst did not induce heterogeneities in the gel. The micrographs exhibited similar aspect, independently of the location of the sample in the gel. The diameters of the tubes were measured with the Analysis software (SIS-Olympus, Münster, Germany). For each experiment, the diameters of more than 200 tubes were measured and averaged. The uncertainty of the measurement was taken equal to the standard deviation. The standard deviations are comprised between 3 and 5 nm; this high value is inherent to the technique: the grain size of the sputtered Pt particles used to shadow the samples is about 2 nm. Then the tubes are more or less deeply embedded which results in a difference between the apparent and real diameters.

Small angle X-ray scattering (SAXS)

Small angle scattering experiments have been performed on two laboratory diffractometers using the CuKα radiation ($\lambda = 1.54$ Å) and different sample to detector distances. These two configurations enabled scattering vectors q to be probed from 0.007 to 1 $Å^{-1}$ (q is defined as $(4\pi/\lambda \sin(\theta/2))$ where λ is the wavelength of the incoming beam and θ is the scattering angle).

The lowest q range was measured with a Rigaku microfocus rotating anode generator (Micromax™-007 HF) operating at 40 kV and 30 mA. The X-ray beam was monochromatized and focused using a confocal Max-Flux Optics™ developed by Osmics, Inc. together with a three pinhole collimation system. Scattered intensity was measured with a 2D multiwire detector located at 1.5 m from the sample. This configuration allowed q vectors to be investigated in the range $0.007\ Å^{-1} < q < 0.16\ Å^{-1}$.

The highest q range was measured on a Nanostar™ diffractometer (Bruker-Anton Paar) operating on a classical sealed tube generator (40 kV, 40 mA). A monochromatic and almost parallel beam was obtained through cross-coupled Göbel mirrors associated with a two pinhole collimator. Scattered photons were collected on a 2D multiwire detector. The sample–detector distance was set to 0.20 m allowing q values to be measured in the range $0.06\ Å^{-1} < q < 1\ Å^{-1}$.

Calibrated mica sheets, one millimetre apart, were used as sample container. Scattering patterns were treated according to the usual procedures for isotropic small angle scattering. Data were radially integrated, and corrected for electronic background, detector efficiency, empty cell scattering, sample transmission and sample thickness. Scattering from the pure solvent was measured separately and subtracted from the sample solution according to its corresponding volume fraction. Intensity was converted into absolute scale using calibrated Lupolen as a standard.

The corrected scattered intensity $I(q)$ which represents the coherent differential cross-section per unit volume of the solute was then analysed using the software developed by NIST Center for Neutron Research.[23]

Analysis of the reacted gels

A gel was prepared, let react and rinsed as described above. It was dissolved in CH_2Cl_2 (5 mL) and the solution was dried under vacuum. The crude was weighed and a small portion (about 5 mg) of it was dissolved in 3 mL THF and volumes of 200 μL of the solution were injected on a chromatography set-up composed of a pump (Shimadzu DGU-20A) operating at a flow of 1 mL min^{-1}, a column PL (granulometry 10 μ), a differential refractometer from Shimadzu (RID6A) and a UV detector from Shimadzu (5SPD 10 Avp). The pure starting materials and final product were injected separately in order to identify the elution times and to calculate the molar extinctions (ε) and refraction increments (dn/dc). The concentrations in the crude were measured from the areas from both the RI and UV traces. The results were in good agreement for both detections. The ratio of final compound/reactants was also measured from the NMR spectra of the crudes by integrating the characteristic peaks of the reagents and products.

Results and discussion

Synthesis of functionalized and reactive tubes

The goal of this study was to synthesize functional analogues of the lead compound **1** that should meet the following two criteria simultaneously: bearing a reactive group for further chemical modification and preserving the ability of forming nanotubes. Since structural models at atomic range resolution are still not available for the tubes formed from **1**, the influence of introducing a chemical group cannot be predicted. However the analogues could be designed according to some simple guidelines. First, the reacting group must be inserted away from the groups that drive the self-assembly: the aromatic part and the amides. Therefore the location that was chosen is the end of the ester alkyl chain. Then the introduced functional group must be small in order not to disturb the packing of the compound inside the tube. Moreover it should not be polar or induce additional H-bonds to avoid additional interaction that could disturb the self-assembly. These rules were also supported by the experimental observation. Analogues with ramified ester chain or with hydroxyl group at the end of the ester chain did not form any tubes. Azide or alkyne were chosen because they fulfill these rules of thumb: they are small, not polar and do not create additional H-bonds. They undergo copper catalyzed

Table 1 Properties of the pure compounds

Compound	Gel formation (gel concentration wt%)	External diameters of tubes/nm
Reactants		
1	G (0.05)	27.5 ± 0.6^b
2	G (0.1)	25.3 ± 3.6^a
3	G (0.04)	27.2 ± 5.0^a 26.5 ± 0.6^b
Products		
4	G (0.85)	31.6 ± 4.3^a
5	P	NA
6	G (0.5)	34.4 ± 0.6^b
7	P	NA

[a] Measured by TEM. [b] Measured by SAXS.

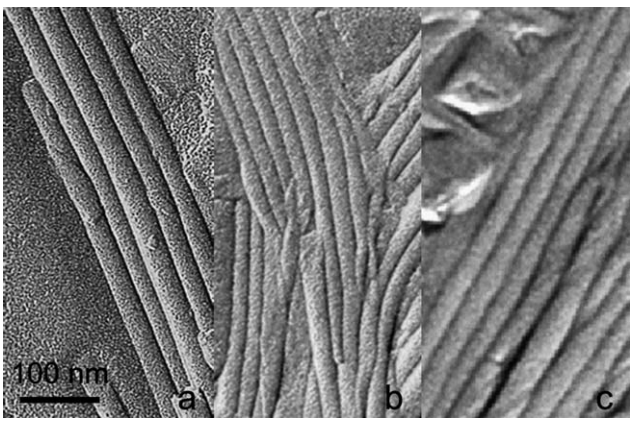

Fig. 2 Freeze fracture TEM of gels of **1** (a), **2** (b) and **3** (c) in cyclohexane (2 wt%).

cycloadditions of alkynes and azides (CuAACs), which is the most famous example of click-chemistry. This reaction proceeds with high yields and is very selective, especially it does not interfere with the other groups of the same molecule. It has been shown that this reaction is effective with large supramolecular species[24] or with polymers.[25,26]

Compounds **2** and **3** were synthesized according to standard methods at the scale of 500 mg.[20] They exhibited a gelator behavior in cyclohexane. The gel concentrations at room temperature were also determined and were found to be in the same order as that of the parent compound **1** (Table 1). The structures of the corresponding gels were studied by freeze fracture electron microscopy, since this technique has proved to be very effective for self-assemblies of related compounds.[19,27–29] The micrographs (Fig. 2) show that the gels are composed of nanotubes that are similar to the ones formed from the parent compound **1** in the same conditions. The lengths are about several micrometres. The diameters were measured from the micrographs on statistically relevant numbers of tubes to yield values of 25.3 ± 3.6 nm and 27.2 ± 5.0 nm for the nanotubes from **2** and **3** respectively.

Set-up and analysis of the reactions directly on nanotubes

The goal of this study is to perform and optimize reactions on self-assembled nanotubes. Since they form organogels, the

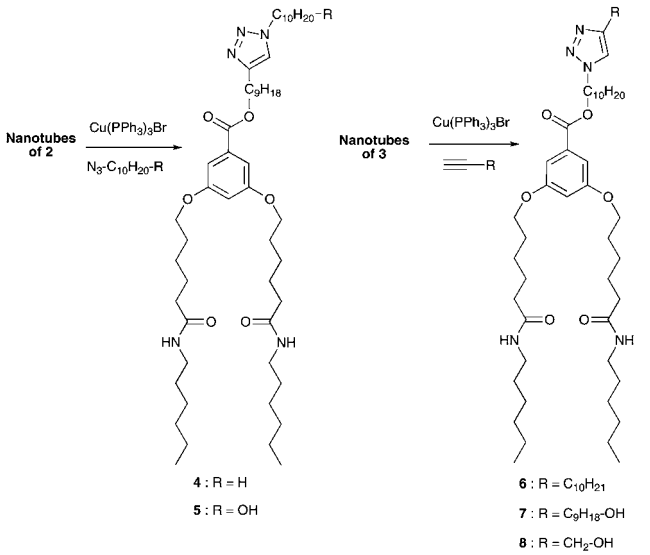

Scheme 2 Reactions performed on the nanotubes; structure of the resulting compounds.

reaction must take place in this highly viscous medium. This condition can be considered as unfavorable, but it has been shown that reactions can take place in organogels,[30,31] including CuAAC.[24,32] The mobility of small molecules in the gel was also measured and found equal to the mobility in solvent.[33,34] The reaction was carried out on the tubes bearing alkyne or azide groups with a free azide or alkyne respectively (Scheme 2). For both tubes (≡-tubes and N_3-tubes), the reaction was tested with an apolar 'clickable' compound (N_3–$C_{10}H_{21}$ or ≡–$C_{10}H_{21}$) and with a polar 'clickable' compound bearing hydroxyl groups (N_3–$C_{10}H_{20}$–OH for ≡-tubes, ≡–C_9H_{18}–OH or ≡–CH_2–OH for N_3-tubes).

The azidoalkane or the alkyne, the copper catalyst and the reducing agent were not mixed with the solutions during the step of gel preparation (*i.e.* nanotubes formation) since they would react with **2** or **3** before they self-assemble into nanotubes. Therefore a solution of these reagents was layered on top of the gels containing the formed nanotubes of **2** or **3** and let diffuse into the gel (Fig. 1). The products of the reacted gels were first analyzed chemically. For this purpose, small portions of the reacted gels were dissolved in chloroform, and the resulting solutions analyzed by NMR and chromatography. The pure products of the reactions (**4**, **5**, **6**, **7**, **8**) were also synthesized independently in solution on a preparative scale and used as standards for the chromatographic experiments to measure

Table 2 Ratio of the products of the reactions on nanotubes and diameters of the resulting nanotubes

Reaction	Products ratio	Diameters of the resulting nanotubes/nm
2 (NT) + N_3–$C_{10}H_{21}$	**4/2** 67/33	24.6 ± 4.1^a
2 (NT) + N_3–$C_{10}H_{20}$–OH	**5/2** 82/18	23.6 ± 3.6^a
3 (NT) + ≡–$C_{10}H_{21}$	**6/3** 14/86	26.6 ± 0.6^b
3 (NT) + ≡–C_9H_{18}–OH	**7/2** 28/72	27.9 ± 4.4^a

[a] Measured by TEM. [b] Measured by SAXS.

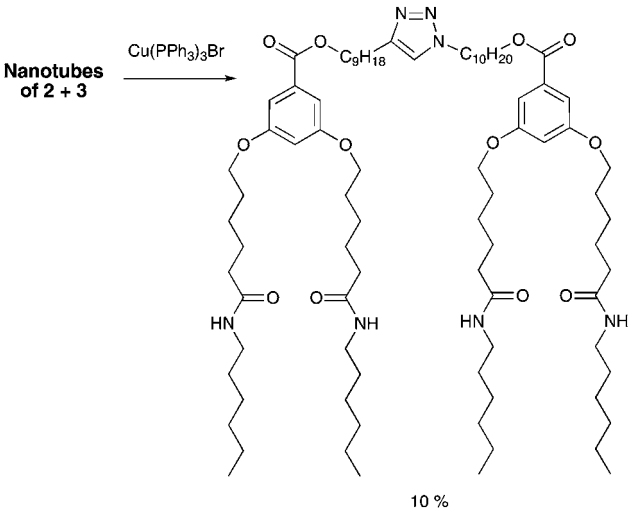

Scheme 3 Reaction of a 1 : 1 mixture of **2** and **3**.

the composition of the reacted gels. The yields are reported in Table 2.

Reaction of gels of **3** with propargylic alcohol led to the formation of **8** with a yield of 70%, but resulted in the dissolution of the gel in the subphase. The propargylic alcohol in excess probably dissolves the products. This dissolution is avoided when N_3–$C_{10}H_{20}$–OH is used as a reagent since it is less polar.

Gels made from a 1 : 1 mixture of **2** and **3** have been prepared and the copper reagent has been let diffuse throughout the gel. The expected chemical reaction is described in Scheme 3. The formation of the product with a yield of 10% is observed. This yield, although modest, is surprisingly high if one takes into account the fact that both reactants are not mobile but engaged in the structure of the tubes. This yield can be attributed to reactions that occur inside the same tube, and thus suggests that nanotubes are not pure **2** tubes or **3** tubes but may be composed of mixtures of both.

Structure of the gels after reaction

The analysis of the products of the reaction proves that the reaction is effective, but cannot tell whether the products are still self-assembled and what is the shape of the eventual self-assemblies. Except for the reaction with propargylic alcohol, the products of the reactions are still forming gels, which suggests that the resulting mixtures form fibrillar aggregates. The morphology of these aggregates was explored by freeze fracture microscopy. The first TEM analysis of the gels was carried out after the gel was rinsed with pure solvent. The micrographs show that nanotubes are present along with many particles that are scattered throughout the samples. These particles have dimensions comprised between 10 and 100 nm and have angular edges (Fig. 3), which suggests that they are crystalline.

Acetylacetone (acac), a copper chelating agent, was added in the cyclohexane during the rinsing steps. This addition cleared the particles, which proves that they are copper by-products.

The addition of acac did not lower the densities of the observed nanoobjects compared with the starting gels, thus showing that the rinsing step does not perturb the self-assembled objects. All

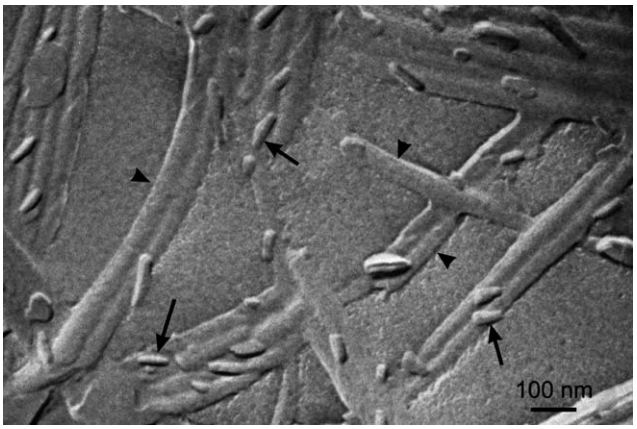

Fig. 3 Freeze fracture TEM of a gel of **2**/C_6H_{12} (2 wt%) reacted with azidodecane before rinsing with acac. Arrowheads: tubes; arrows: particles that disappear when acac is used in the rinsing solution.

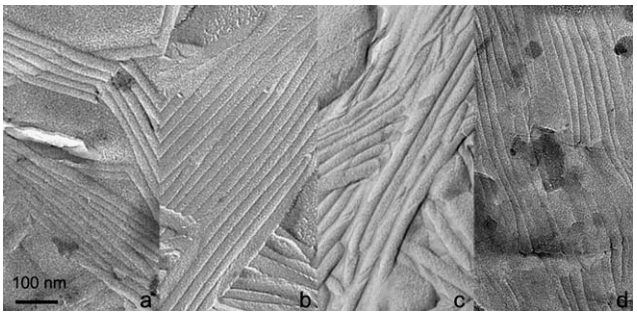

Fig. 4 Freeze fracture TEM of the gels after reaction: (a) **2** + N_3–$C_{10}H_{21}$; (b) **2** + N_3–$C_{10}H_{20}$–OH; (c) **3** + ≡–C_9H_{18}–OH; and (d) **3** + ≡–$C_{10}H_{21}$.

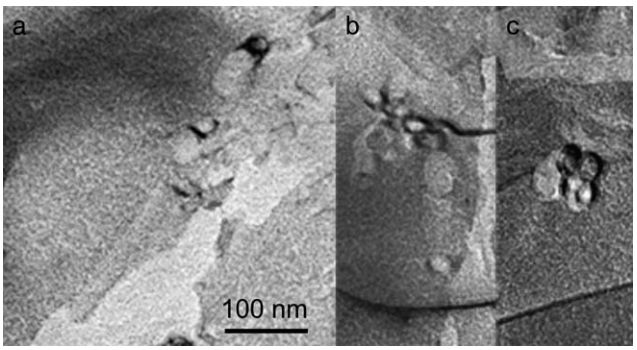

Fig. 5 Freeze fracture TEM showing the cross-sections of the self-assemblies of: (a) reacted gels of **2** + N_3–$C_{10}H_{21}$ and (b and c) pure **4**.

the samples studied by freeze fracture TEM (**2** + N_3–$C_{10}H_{21}$, **2** + N_3–$C_{10}H_{20}$–OH, **3** + ≡–$C_{10}H_{21}$, **3** + ≡–C_9H_{18}–OH) are composed exclusively of nanotubes (Fig. 4).

In every case, a small number of the freeze fractures occur perpendicularly to the objects and show the cross-sections of the objects. Examples of the corresponding micrographs are shown in Fig. 5. Those micrographs exhibit the hole in the sections and prove that these objects are tubes and not plain cylinders. Definite proof of the tubular shape is given below by the SAXS experiments.

The density of the objects in each sample preparations is the same as in the initial gels, which shows that the products **4**, **5**, **6** and **7** do not dissolve or segregate but remain self-assembled into nanotubes. Since the reaction is limited by the slow diffusion of one of the reagents and the catalyst, the structure of the gel may vary with the distance from the diffusing top layer. The gels were analyzed at different heights: the same structures and tube densities were observed, which showed that reaction times were long enough to afford homogeneous gels. The diameters of the tubes resulting from the reaction in the gel of **2** with azidodecane or azidodecanol are resp. 24.6 ± 4.1, 23.6 ± 3.6 nm which are close to the diameters of the initial tubes of **2** (25.3 ± 3.6 nm). Also the diameters of the tubes obtained by reaction of **3** with undecynol (27.9 ± 4.4 nm) are close to the ones of the tubes before reaction (27.2 ± 5 nm).

Given the rather small transformation rate of the reaction in the gels of **3** with dodecyne (14%) one can expect only a small change in the radii of the tubes. Microscopic measurements have a high uncertainty (>3 nm) hence small changes cannot be detected. For the case of compound **3**, the diameters of the tubes before and after reaction were measured by SAXS studies. This technique provides an average measurement on the whole sample and is non-destructive, which is necessary to corroborate and refine the microscopic observations.

The scattered intensities $I(q)$ are presented in Fig. 6 in the Kratky representation: $q^2I(q)$ *vs.* q. Scattering patterns exhibit sharp oscillations in the low q region which are characteristic of the cross-section of the particles. The intensities were fitted by modelling the particles as infinite hollow cylinders, with a constant and homogeneous scattering length density. For a pure monodisperse nanotubes population, in the absence of inter-tube correlation, the scattered intensity (cm^{-1}) can be expressed as

$$I(q) = \phi_V \Delta\rho^2 V_p P(q) \quad (1)$$

where ϕ_V is the volume fraction of the particles, $\Delta\rho$ is the difference in scattering length density (cm^{-2}) of the particle and the solvent, V_P is the volume (cm^3) of the particle and $P(q)$ the form factor of the hollow cylinders.

Under the assumption that $qL \gg 1$ (with L the length of the nanotubes), $P(q)$ can be written as a function of the external radius r_{ext} and the wall thickness e:[35]

$$P(q) = \frac{\pi}{qL}\left[\frac{(r_{ext}J_1(qr_{ext}) - (r_{ext} - e)J_1(q(r_{ext} - e)))}{qe(r_{ext} - e/2)}\right]^2 \quad (2)$$

In this expression, J_1 is the Bessel function of first kind and first order.

The typical oscillations, visible q values lower than 0.16 $Å^{-1}$, were measured on the rotating anode diffractometer, but could not be observed at higher q values due to the poorer resolution of the set-up. For that reason, the curves are presented only below 0.25 $Å^{-1}$. For some of the measurements, the exact positions of the maxima and the minima slightly mismatched the best-fit expectations from eqn (2). We explain this behaviour as a consequence of the bunching of several nanotubes.[36] The fit quality especially in the low q region was improved by considering the simple case of bunching two parallel tubes in close contact. Under such a condition, the scattered intensity has to be multiplied by

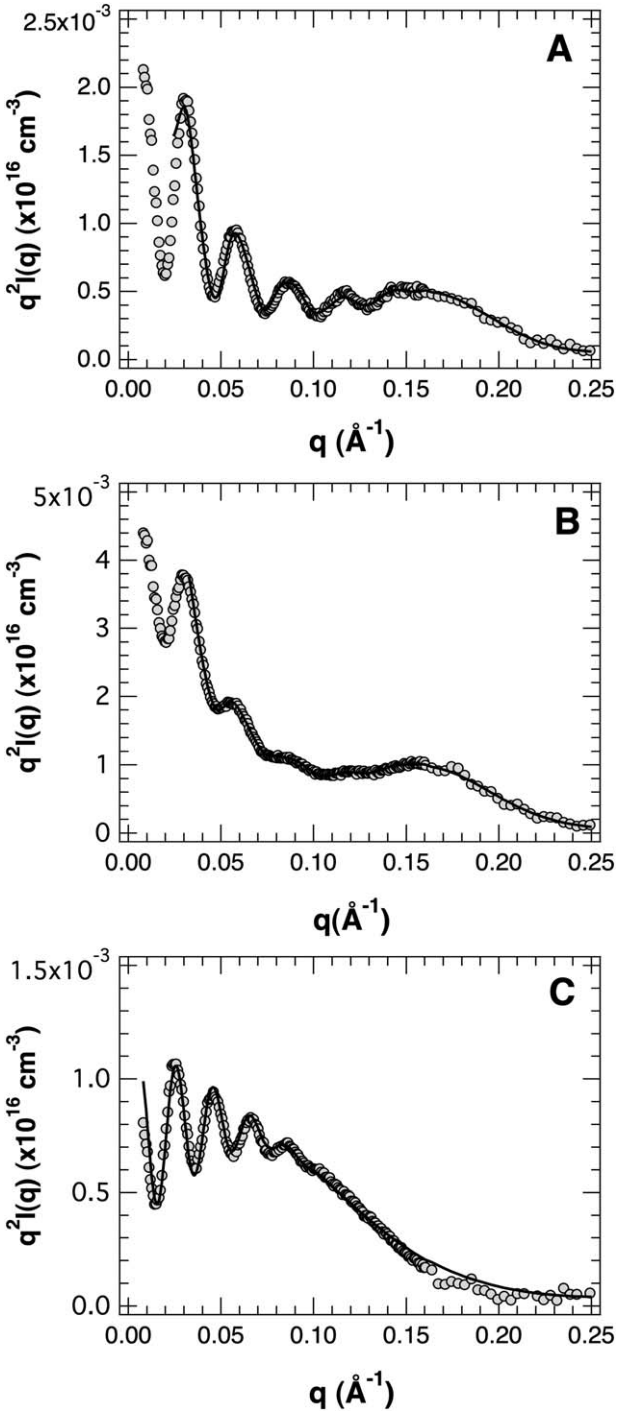

Fig. 6 SAXS: Kratky plots $q^2I(q)$ *vs.* q for the gels at 2 wt%: (A) **3**; (B) reacted gel **3** + ≡–$C_{10}H_{21}$; and (C) **6**. Dots: experimental curves. Solid lines: theoretical fits (see text).

$$(1 + J_0(2qr_{ext})) \quad (3)$$

where J_0 is the Bessel function of first kind and zero order. The oscillations of the scattered intensities observed at the low q-range are quite well accounted by eqn (2) and (3) which show that they are characteristic of the tubular shape of the particles, which is consistent with the TEM observations. The radial polydispersity of the tubes can be measured from the fits. Sharp

Table 3 Structural parameters extracted from SAXS analysis

Sample	External diameters $2r_e$/nm	Thicknesses of the wall/nm	Deviation 2σ of the diameters distributions/nm
3	26.5 ± 0.6	2.9 ± 0.3	0.11 ± 0.02
3 (NT) + ≡–$C_{10}H_{21}$	26.6 ± 0.6	3.1 ± 0.3	0.14 ± 0.02
6	34.4 ± 0.6	3.4 ± 0.3	0.11 ± 0.02

oscillations indicate a low polydispersity while smoothed oscillations indicate a narrow one. We have considered a log-normal distribution of the radii (associated with a constant wall thickness) with a deviation 2σ and took into account the resolution smearing effects. The results of the measured diameters and deviation are summarized in Table 3.

The structural parameters are very close for the tubes before and after reaction (entries **3** and **3** (NT) + ≡–$C_{10}H_{21}$). The outer diameters are equal within an uncertainty less than 2% of the diameter. The observed differences are slight increases of the thickness and of the dispersity after reaction. These parameters are very strong evidence that no major structural changes have occurred during the reaction.

As already observed for **1** in *trans*-decalin,[36] we also note the presence of a broad maximum (in Kratky representation) located around 0.16 $Å^{-1}$ for **3** and the reacted gel **6/3**. This additional intensity cannot be explained on the basis of eqn (2) even combined with eqn (3). The origin of this contribution is not clear but involves a characteristic distance of 39 Å, and could be a Bragg peak due to a local organisation inside the nanotube walls. Eqn (2) and (3) describe correctly the scattering by the hollow cylinders but do not account for internal order. This peak could also arise from the presence of other small aggregates, different from the hollow cylinders considered above, but they were not visible from the microscopy experiments. Another contribution was then added to the theoretical expression in order to account for this extra scattering.[30] This additional peak is observed at the same q-value in both gels of **3** and the reacted gel **3/6**, which shows that no major structural change occurred during the reaction.

Thermoreversibility of the formed nanotubes

The new nanotubes that we have observed after the reaction in the gel were obtained from the direct modification of nanotubes consisted of self-assembled molecules. They are stable over periods of a few months. Is this stability due to the fact that the new nanotubes exist in a stable self-assembled state of the reacted compounds? In order to answer the question, the reacted tubes were heated until complete dissociation and cooled again to check whether the tubes reform. Under these conditions the gels produced by reactions of nanotubes of **2** and $C_{10}H_{21}$–OH or nanotubes of **3** and ≡–C_9H_{18}–OH do not reform identically. Upon heating, compound **5** (resp. **7**) melts and the liquid demixes from the solution and precipitates. The supernatant solution forms a gel of unreacted **2** (resp. **3**) upon cooling. The comparison has been made with the pure compounds **5** and **7**. When they are heated in C_6H_{12} they melt and do not mix with the solvent and precipitates upon cooling. Heating a mixture of **5** and **2** in the same proportions (82/18) as found in the gels after reaction led to the same precipitation of pure **5**. These experiments prove that the nanotubes observed after reaction by diffusion cannot be reassembled from their constituting molecules.

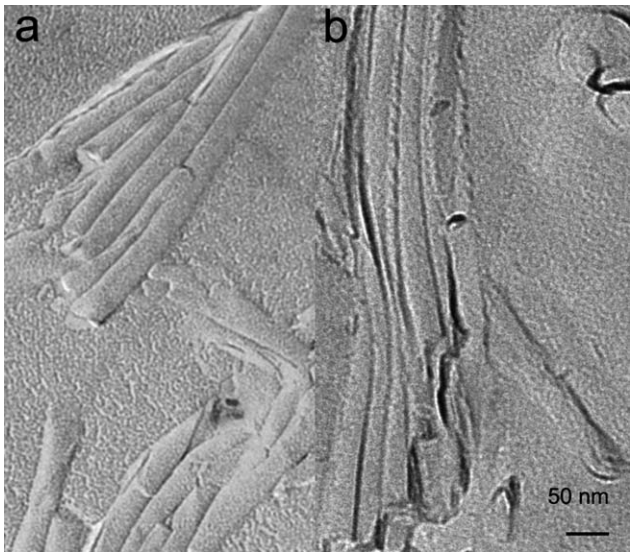

Fig. 7 Freeze fracture TEM of the gels of the pure final compounds in C_6H_{12} (2 wt%): (a) **4** and (b) **6**.

The gels generated by the reactions of nanotubes of **2** + N_3–$C_{10}H_{21}$ or nanotubes of **3** + ≡–$C_{12}H_{25}$ can reform. The pure compounds **4** and **6** self-associate in alkanes to form organogels with gel concentrations of 0.85 and 0.5% respectively. Freeze fracture microscopy of the gels of pure **4** (Fig. 7) shows that this compound self-assembles into nanotubes with diameters of 31.6 nm, significantly larger than those of the nanotubes formed in the reaction **2** + N_3–$C_{10}H_{21}$ (25.3 ± 3.6 nm) although these reacted nanotubes contain 67% of **4**.

The diameters of the nanotubes of **6** were measured by SAXS (Fig. 6C) and were found equal to 34.4 ± 0.6 nm, which is also larger than that of the tubes yielded by the reaction **3** + ≡–$C_{12}H_{25}$ (26.2 ± 0.6 nm). In this case, the final mixture contains only 14% of **6** and this low proportion is expected to induce a slight change in the average, but yet should be detected by SAXS on the reacted gels. But the results (Table 3) show no significant increase. Moreover, the large peak observed at 0.16 $Å^{-1}$ in the starting tubes of **3** before and after reaction is shifted to lower q values (0.06 $Å^{-1}$), which reflects a change of the order inside the tubes. These particular features confirm that the tubes formed directly from **6** have a different structure from the ones formed by reaction **3** + ≡–$C_{10}H_{21}$.

These comparisons show that the new nanotubes formed from the reaction on tubes of **2** or **3** are different from the objects that spontaneously form from their constituting molecules. The constituents spontaneously form precipitates or tubes with different size. These phenomena, summarized in Scheme 4, prove that the tubes obtained by click-chemistry are metastable, even if they are kinetically stable during several months.

Their formation can be explained by the fact that the nanotubes are formed from hot solution and 'frozen' into a non-dynamic structure at room temperature. They also have a crystalline structure as shown previously[19] by WAXS performed with

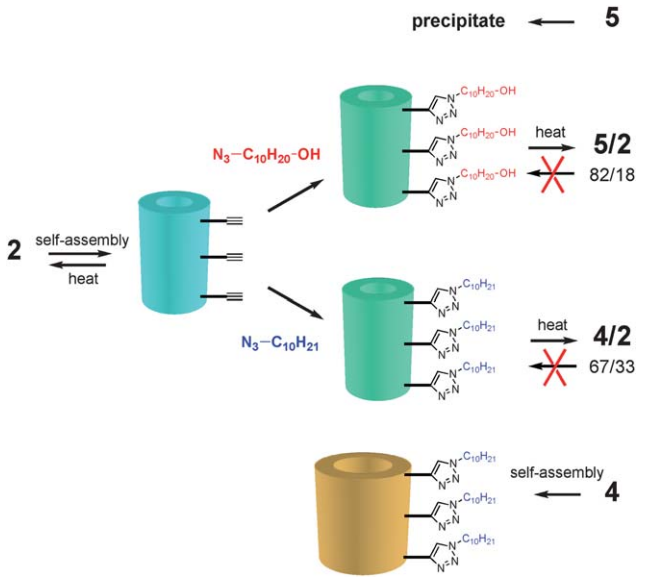

Scheme 4 Summary of the conversions of compound **2** and derivatives. The same kind of scheme could be drawn for derivatives of **3**.

1 and confirmed here by the presence of the peaks around 0.16 $Å^{-1}$ with **3** and **3** + ≡–$C_{12}H_{25}$. The molecules inside the tubes can react by their alkyne or azide groups quite fast, but they cannot evolve fast enough toward a larger but more stable tube or a solid. This behaviour offers the possibility to elaborate functional self-assembled nanotubes from constituents that do not spontaneously self-assemble into nanotubes. Hence it avoids a lengthy trial and error process to discover new nanotubes.

Conclusions

Although the structures of the self-assembled nanotubes are not known at a molecular level, it is possible to insert reactive groups on self-assembled nanotubes. This addition is performed by chemical modification of the constituting compounds before self-assembly. It does not drastically alter the self-assembling pattern when simple rules are followed: the introduced groups must be small and non-polar. Azides and alkynes were found to be suitable. Both groups can react by click chemistry. The resulting analogues undergo this reaction even under their self-assembled state and the resulting yields are quite high for most of the conducted reactions. This high reactivity shows that probably the reactive groups are turned and exposed toward the outside of the tubes.

We have proved that the tubes obtained after the click reactions have the same size as the starting ones. When they are dissociated by heat, the resulting molecules do not re-assemble by cooling. Therefore the overall strategy provides a means to form new nanotubes from compounds that do not spontaneously self-assemble into nanotubes. We will take advantage of this fact to prepare tubes functionalized with new groups, while avoiding lengthy syntheses and trials to screen new functional nanotubes.

Acknowledgements

This work was supported by a fellowship from the Région Alsace (T.-T.-T. Nguyen) and a grant from the International Center for Frontier Research in Chemistry, Strasbourg. We thank G. Fleith for the SAXS measurements.

References

1 S. Iijima and T. Ichihashi, *Nature*, 1993, **363**, 603–605.
2 D. S. Bethune, C. H. Klang, M. S. de Vries, G. Gorman, R. Savoy, J. Vazquez and R. Beyers, *Nature*, 1993, **363**, 605–607.
3 S. Iijima, *Nature*, 1991, **354**, 56–58.
4 R. H. Baughman, A. A. Zakhidov and W. A. de Heer, *Science*, 2002, **297**, 787–792.
5 R. Singh, D. Pantarotto, L. Lacerda, G. Pastorin, C. Klumpp, M. Prato, A. Bianco and K. Kostarelos, *Proc. Natl. Acad. Sci. U. S. A.*, 2006, **103**, 3357–3362.
6 R. Singh, D. Pantarotto, D. McCarthy, O. Chaloin, J. Hoebeke, C. D. Partidos, J.-P. Briand, M. Prato, A. Bianco and K. Kostarelos, *J. Am. Chem. Soc.*, 2005, **127**, 4388–4396.
7 M. Moniruzzaman and K. I. Winey, *Macromolecules*, 2006, **39**, 5194–5205.
8 D. Tasis, N. Tagmatarchis, A. Bianco and M. Prato, *Chem. Rev.*, 2006, **106**, 1105–1136.
9 H. Fenniri, B.-L. Deng and A. E. Ribbe, *J. Am. Chem. Soc.*, 2002, **124**, 11064–11072.
10 P. Ringler, W. Muller, H. Ringsdorf and A. Brisson, *Chem.–Eur. J.*, 1997, **3**, 620–625.
11 E. M. Wilson-Kubalek, R. E. Brown, H. Celia and R. A. Milligan, *Proc. Natl. Acad. Sci. U. S. A.*, 1998, **95**, 8040–8045.
12 C. Valery, M. Paternostre, B. Robert, T. Gulik-Krzywicki, T. Narayanan, J. C. Dedieu, G. Keller, M. L. Torres, R. Cherif-Cheikh, P. Calvo and F. Artzner, *Proc. Natl. Acad. Sci. U. S. A.*, 2003, **100**, 10258–10262.
13 R. Oda, F. Artzner, M. Laguerre and I. Huc, *J. Am. Chem. Soc.*, 2008, **130**, 14705–14712.
14 W. Helfrich, *J. Chem. Phys.*, 1986, **85**, 1085–1087.
15 U. Seifert, J. Shillcock and P. Nelson, *Phys. Rev. Lett.*, 1996, **77**, 5237.
16 J. V. Selinger and J. M. Schnur, *Phys. Rev. Lett.*, 1993, **71**, 4091.
17 J. V. Selinger, M. S. Spector and J. M. Schnur, *J. Phys. Chem. B*, 2001, **105**, 7157–7169.
18 J. V. Selinger, F. C. MacKintosh and J. M. Schnur, *Phys. Rev. E: Stat. Phys., Plasmas, Fluids, Relat. Interdiscip. Top.*, 1996, **53**, 3804–3818.
19 N. Diaz, F. X. Simon, M. Schmutz, M. Rawiso, G. Decher, J. Jestin and P. J. Mésini, *Angew. Chem., Int. Ed.*, 2005, **44**, 3260–3264.
20 T.-T.-T. Nguyen, F.-X. Simon, M. Schmutz and P. J. Mésini, *Chem. Commun.*, 2009, 3457–3459.
21 R. Huisgen, in *1,3-Dipolar Cycloaddition Chemistry*, ed. A. Padwa, Wiley-Interscience, New York, 1984, vol. 1, pp. 1–176.
22 H. C. Kolb, M. G. Finn and K. B. Sharpless, *Angew. Chem., Int. Ed.*, 2001, **40**, 2004–2021.
23 S. Kline, *J. Appl. Crystallogr.*, 2006, **39**, 895–900.
24 D. D. Diaz, K. Rajagopal, E. Strable, J. Schneider and M. G. Finn, *J. Am. Chem. Soc.*, 2006, **128**, 6056–6057.
25 R. S. Wolfgang and H. Binder, *Macromol. Rapid Commun.*, 2007, **28**, 15–54.
26 J. F. Lutz, *Angew. Chem., Int. Ed.*, 2007, **46**, 1018–1025.
27 M. Schmutz and P. J. Mésini, in *Handbook of Cryopreparation Methods for Electron Microscopy*, ed. A. Cavalier, D. Spehner and B. M. Humbel, Taylor & Francis, CRC press, New York, 2008, pp. 411–430.
28 R. Schmidt, M. Schmutz, M. Michel, G. Decher and P. J. Mésini, *Langmuir*, 2002, **18**, 5668–5672.
29 R. Schmidt, F. B. Adam, M. Michel, M. Schmutz, G. Decher and P. J. Mésini, *Tetrahedron Lett.*, 2003, **44**, 3171–3174.
30 J. R. Moffat, I. A. Coates, F. J. Leng and D. K. Smith, *Langmuir*, 2009, **25**, 8786–8793.
31 J. F. Miravet and B. Escuder, *Org. Lett.*, 2005, **7**, 4791–4794.
32 D. D. Díaz, J. J. M. Tellado, D. G. Velázquez and Á. G. Ravelo, *Tetrahedron Lett.*, 2008, **49**, 1340–1343.
33 A. Masuda, K. Ushida, H. Koshino, K. Yamashita and T. Kluge, *J. Am. Chem. Soc.*, 2001, **123**, 11468–11471.
34 F. Galindo, M. I. Burguete, R. Gavara and S. V. Luis, *J. Photochem. Photobiol., A*, 2006, **178**, 57–61.
35 J. M. Deutch, *Macromolecules*, 1981, **14**, 1826–1827.
36 D. Dasgupta, Z. Kamar, C. Rochas, M. Dahmani, P. Mesini and J. M. Guenet, *Soft Matter*, 2010, **6**, 3573–3581.

